PHYSICAL REVIEW B VOLUME 27, NUMBER 2 15 JANUARY 1983

Electronic structures of Co(II) and Co(III) impurities in cubic perovskite hosts

F. M. Michel-Calendini and P. Moretti
Laboratoire d'Electronique Bâtiment 203, Université Lyon-1 43, Boulevard du 11 Novembre 1918, 69622 Villeurbanne Cedex, France
(Received 21 June 1982; revised manuscript received 6 October 1982)

The spin-polarized option of the multiple-scattering $X\alpha$ method is used to obtain the electronic structures of divalent and trivalent cobalt ions in $SrTiO_3$ and $BaTiO_3$ samples. Various clusters account for the different charge-compensation mechanisms (oxygen vacancies, fluorine ions) and different spin configurations are considered for Co(II) and Co(III) centers. Transition-state computations are carried out to get the various multiplet levels of Co(II) and CO(III) cubic centers. The high-spin $^5T_{2g}$ and the low-spin $^1A_{1g}$ terms are, respectively, the Co(III) ground terms in $BaTiO_3$ and $SrTiO_3$ hosts. The 10Dq crystal-field parameter of Co(III) increases from 1.9 eV ($BaTiO_3$) to 2.1 eV ($SrTiO_3$). In the light of $X\alpha$ energy diagrams, the possible interpretations of the absorption spectra relevant to Reimeika $BaTiO_3$:Co and $SrTiO_3$:Co crystals are reviewed.

I. INTRODUCTION

Perovskitelike oxides doped with $3d$ transition-metal ions have been extensively studied in the past few years. The doping effects on their physical properties are probably connected with the equilibrium-defect distribution which is related to the ambiant oxygen partial pressure, the temperature, and the impurities present from the preparation.[1] Moreover, many works[2,3] (and references herein) describe how oxidizing and reducing annealing treatments change the nature of the transition-metal related centers. Optical, electron paramagnetic resonance (EPR), and electrical experiments are the main tools to investigate the nature of the impurities and of their associated defects.

Concerning the Co impurities trapped in $BaTiO_3$ or $SrTiO_3$ crystals, the available experimental data[3–11] show many similar features with the results about the Fe impurities in the same hosts.[6–15]

(a) These transition ions enter as substitutions at the Ti^{4+} site.

(b) Several nominal ionicities are observed under irradiation or thermal treatments[3,14] and the resulting chromic properties seem to depend on similar electronic processes.[6,13]

(c) The charge-compensation mechanisms involve mainly oxygen vacancies (V_O) for doping ions with valencies smaller than four,[12] and with additional charge compensation by fluorine ions arising in $BaTiO_3$ crystals grown by the KF flux method.[10,11]

(d) Several ground terms are possible for a given nominal ionicity of the transition ion, according to its crystalline environment, as shown by the following examples: In $SrTiO_3$, the cubic Fe^{4+} center has a spin $S=0$ while the axial Fe^{4+}-V_O one is paramagnetic with $S=2$ (Ref. 15); the Co(III) ion is diamagnetic in $SrTiO_3$ (Ref. 7) and paramagnetic in $BaTiO_3$ ceramics.[5]

Despite numerous experimental results available for these materials, theoretical investigations of their electronic structures have received little attention in the literature. Some recent molecular-orbital computations exist for Fe doping ions,[16,17] but up to now, the main way to get some insight into the energy diagrams relevant to Co-doped perovskites is to refer either to calculations reported for bulk crystals like CoO (Refs. 18 and 19) or to results provided by crystal-field models.[20]

Thus it is worthwhile to undertake a series of molecular-orbital computations on $BaTiO_3$:Co and $SrTiO_3$:Co crystals, with the use of the self-consistent-field $X\alpha$ spin-unrestricted method.[21]

In Sec. II of this work, the ground-state eigenvalues relevant to the clusters representative of Co ions and of their associated defects are reported with a special emphasis on the effects of the spin configuration. In Sec. III, the absorption spectra and the ground terms are discussed in the light of the energy diagrams, while Sec. IV is a summary of the main results of this work.

II. GROUND-STATE EIGENVALUES AND IMPURITY LEVELS

A. Theoretical background

1. *Different clusters representative of Co-doped crystals*

The chemical analyses carried out on Reimeika $BaTiO_3$:Co samples[10,11] show different charge-compensation mechanisms according to the impurity concentration: One oxygen vacancy is associated to a Co ion when the atomic Co percentage is less than 0.2% and two fluorine F^- ions are associated to Co(II) for higher concentrations. This leads to many possible impurity centers, the most significant being: Ti^{4+}-F (TiO_5F^{7-} cluster), Ti^{4+}-V_O (TiO_5^{6-}), Co^{n+} (CoO_6^{n-12}), Co^{n+}-V_O (CoO_5^{n-10}), Co^{n+}-F (CoO_5F^{n-11}), and Co^{2+}-F_2 ($CoO_4F_2^{8-}$), with $n=2$ and 3. The centers involving F ions are specific to Reimeika crystals. In the following we will denote the molecular complex by its associated center in order to simplify. We worked in the paraelectric phase of $BaTiO_3$ and $SrTiO_3$ which gives the cluster-point groups O_h [one species in the center; Co(II), for instance] and C_{4v} (two different species like Co and V_O, for example). The energy diagrams relevant to these clusters are compared to the Ti^{4+} cluster (TiO_6^{8-} cubic cluster), which is assumed to be representative of the undoped material.[22] The localization of the impurity levels in the intrinsic Ti^{4+} gap are obtained as in the case of Fe and Fe-V_O defects.[16,17]

2. *Ground-state configurations*

The electronic structure of a $3d$ ion embedded in a crystal host is mainly dependent on two parameters of equal importance: (i) the nominal ionicity and (ii) the ground term of the impurity.[16] These parameters are usually obtained from experimental data. The cobalt ion may exist under several ionicities and spin configurations in perovskite crystals. For instance, Richter *et al.*[23] found Co(II), Co(III), and Co(IV) species with various ground terms in $LaCoO_3$ crystals depending on temperature. Main *et al.*[24] discuss more specifically the high-spin (HS) and low-spin (LS) configurations of Co(III) oxides. In $SrTiO_3$, Co(III) is found in its diamagnetic state $d\epsilon^6$ ($^1A_{1g}$ ground term) (Ref. 7) while in $BaTiO_3$ ceramics, the HS configuration $d\epsilon^4 d\gamma^2$ ($^5T_{2g}$) appears to be the most probable from magnetic susceptibility measurements.[5] These latter observations receive an indirect theoretical justification from the EPR measurements of the cubic parameter a of Fe^{3+} substituted in cubic oxides.[25] Indeed, the a value which is relevant to $BaTiO_3$:Fe is reduced by about 30% relative to the values obtained for MgO:Fe or $SrTiO_3$:Fe crystals. This suggests that the 10Dq crystal-field energy is lowered when a $3d$ impurity is trapped in $BaTiO_3$ rather than in $SrTiO_3$. Then, from considerations on the d^6

TABLE I. $X\alpha$ parameters and atomic positions relevant to a cubic cell parameter $d=4$ Å.

Atomic positions in a.u.[a]
Ti or Co: clusters without V_O(0,0,0); C_{4v} clusters with a V_O(0,0,0.378)
O_i ($i=1-6$ in cubic clusters): ($\pm$3.78,0,0); (0,$\pm$3.78,0);(0,0,$\pm$3.78)
For axial centers, V_O or F are substituted at the oxygen site (0,0, + 3.78)
Sphere radii in a.u.[a]
TiO_6, TiO_5F, TiO_5: $R_{Ti}=2.00$, $R_0=1.78$, $R_F=1.78$, $R_{V_O}=1.78$
CoO_6, CoO_5F, CoO_5: $R_{Co}=1.96$, $R_0=1.82$, $R_F=1.78$, $R_{V_O}=1.82$
All clusters: $R_{OS}=R_{WS}=5.6$
α parameters
$\alpha_{Ti}=0.71698$, $\alpha_0=0.74447$; $\alpha_F=0.73732$, $\alpha_{V_O}=\alpha_0$
$\alpha_{Co}=0.71018$
$\alpha_{IS}=\alpha_{OS}=$weighted averaged values on atomic α
Watson sphere (WS) charges in $\lvert e \rvert$ units
$q(TiO_6)=8.5$; $q(Co^{2+}O_6)=10.5$; $q(Co^{3+}O_6)=9.5$.
$q(TiO_5F)=7.5$; $q(Co^{2+}O_5F)=9.5$; $q(Co^{3+}O_5F)=8.5$.
$q(TiO_5)=6.5$; $q(Co^{2+}O_5)=8.5$; $q(Co^{3+}O_5)=7.5$.

[a]The parameters relevant to $SrTiO_3$ ($d=3.9$ Å) are obtained from the preceding ones by multiplying by 0.975.

energy-level pattern[20] of Tanabe and Sugano (hereafter denoted TS), the LS Co^{III+} configuration is expected for $SrTiO_3$:Co(III) (with $Dq|B>2$), while the HS Co^{3+} one becomes more probable in $BaTiO_3$:Co(III). $X\alpha$ transition-state computations of the term energies of Co(III) in the $SrTiO_3$ and $BaTiO_3$ hosts confirm these hypotheses, as will be seen in Sec. III.

3. $X\alpha$ parameters

The following spin configurations of Co(II) and Co(III) species have been investigated: LS Co^{II+} ($d\epsilon^6 d\gamma^1\,{}^2E_g$), LS Co^{III+} ($d\epsilon^6\,{}^1A_{1g}$), HS Co^{2+} ($d\epsilon^5 d\gamma^2\,{}^4T_{1g}$), and HS Co^{3+} ($d\epsilon^4 d\gamma^2\,{}^5T_{2g}$).

The $X\alpha$ parameters, given in Table I, have been chosen as described in earlier works.[16,17,22] Let us summarize. The distances between the center of the M sphere (M=Co or Ti), and the ones of the O_i oxygen spheres situated at the octahedron's corners ($i=1-6$), are, respectively, of 2 Å for $BaTiO_3$ and of 1.95 Å for $SrTiO_3$. When an oxygen vacancy is present in the cluster, an empty sphere having the same radius as the oxygen sphere is centered at the V_O site; moreover, the M sphere is shifted by a 0.2-Å length towards the V_O site along the C_{4v} symmetry axis in order to account for the results of Siegel and Müller.[26]

The atomic-sphere radii of the cubic centers are chosen according to the touching-sphere requirement and the Norman's procedure.[27] These radii remain unchanged in the calculations concerning the C_{4v} clusters. The barium and strontium ions are treated as ionic charges modifying the electronic levels by means of the total charge of the cluster. The electronic charge environment of the cluster is simulated by a Watson sphere (WS) with the same radius as the outer sphere (OS); the WS bears a positive charge equal to the absolute value of the one of the cluster, plus one-half unit, which allow us to obtain bound levels for the whole conduction band.

Calculations are carried out including partial waves up to $l=1$ for O (or F) spheres and $l=3$ for M spheres and the extramolecular region. The orbitals relevant to the deeper states O 1s, M 1p, M 2s, M 2p are treated in the "thawed" core approximation[28]: They keep their atomic character, but their charge distribution and energies are varied during the self-consistency procedure. A $\pm 10^{-4}$ Rydberg convergence criterium is chosen for each energy level. The statistical-exchange parameters α relevant to atomic-sphere regions are taken from Schwarz's tabulation,[29] and weighted averages of the atomic values are used in the interatomic (IS) and OS regions.

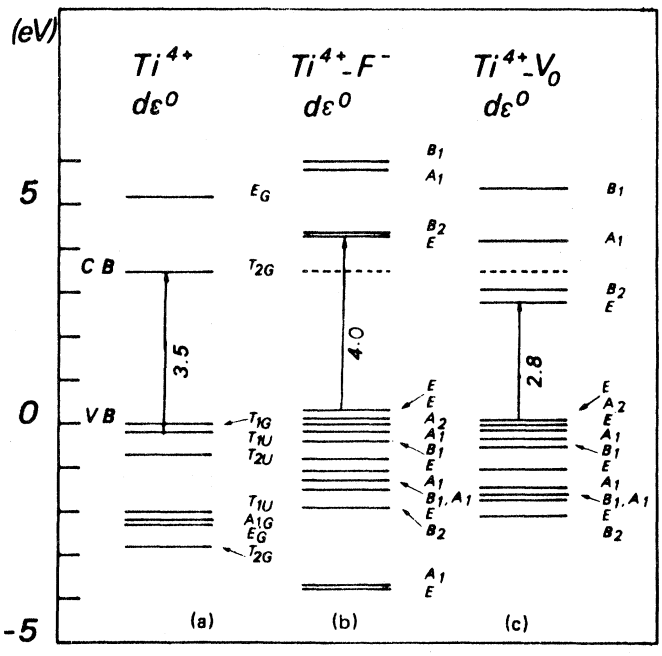

FIG. 1. Ground-state $X\alpha$ eigenvalues for cubic and axial Ti^{4+} centers: (a) TiO_6^{8-} cluster (Ti^{4+} center, representative of the undoped cubic $BaTiO_3$ crystal). (b) TiO_5F^{7-} cluster (Ti^{4+}-F C_{4v} center). (c) TiO_5^{6-} cluster (Ti^{4+}-V_O C_{4v} center). (The first allowed transitions and the corresponding $X\alpha$ eigenvalue differences are pictured by vertical arrows, with energy values in eV.)

B. Energy-level diagrams

Ground-state $X\alpha$ eigenvalues relevant to Co(Ti) $3d$ and O(F) $2p$ states are plotted in Figs. 1—3 and the molecular diagram representative of the undoped crystal (Ti^{4+} center) is given in Fig. 1(a) for the $BaTiO_3$ host. The $Ti^{4+}O_{2p}$ t_{1g} state is chosen as zero-energy reference level [valence band (VB)], while the Ti^{4+} t_{2g} one is the conduction-band edge (CB). For the other clusters, the $t_{1g}\uparrow$ (cubic center) or the $a_2\uparrow$ (axial center) states have been scaled to the VB level since they present the same pure oxygen character, independent of the nature of the central ion. The weak-spin splitting between the up- and down-spin t_{1g} (or a_2) states allows us to choose arbitrarily the up-spin level as reference for the VB top in spin-polarized configurations. A dotted line shows the CB level in all the diagrams for a better visualization of the impurity states located inside the intrinsic gap.

The diagrams associated with the 3.9-Å $SrTiO_3$ parameter do not differ appreciably from those reported in Figs. 1—3. This allows a common description of the electronic behavior of impurity centers in cubic $BaTiO_3$ and $SrTiO_3$ hosts.

1. Cubic centers

The importance of the spin configurations for a given ionicity of Co ion is clearly depicted by the differences between the diagrams of Figs. 2(a) and 2(b) for Co(II) and of Figs. 3(a) and 3(b) for Co(III). For instance, the LS Co^{III+} center can not have a charge-transfer band at energies less than the band gap value as the only empty $d\gamma e_g$ level is localized near CB, while Co^{3+} has a partly filled $t_{2g}\downarrow$ state in the middle of the gap, allowing $t_{1u}\downarrow(t_{2u}\downarrow)\rightarrow t_{2g}\downarrow$ transitions to begin at about 2 eV. The Figs. 2(a) and 3(a) (LS) or 2(b) and 3(b) (HS) show that Co $3d$ levels lower inside the gap as the nominal ionicity of Co ion increases. The downwards shifts of the impurity states according to the valencies have already been noticed for the Fe centers[16] but they depend also on the change of the spin configuration from one ionicity to the other.

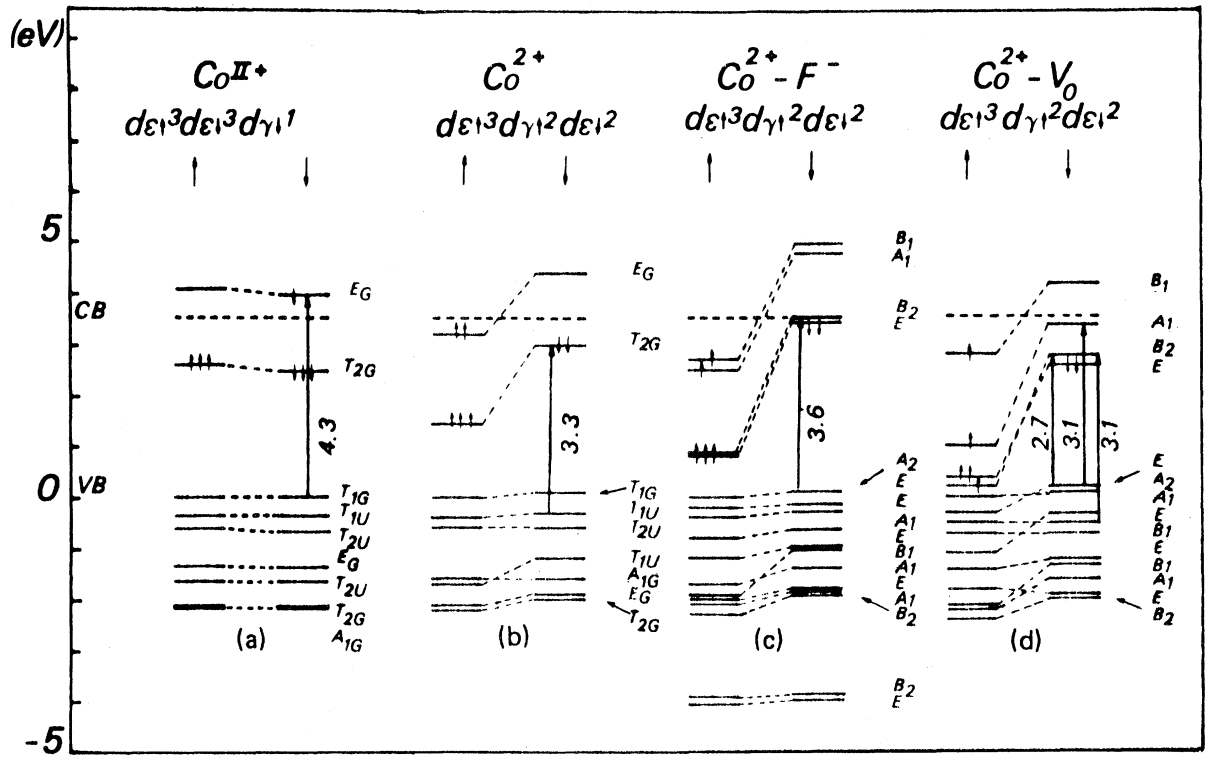

FIG. 2. Ground-state $X\alpha$ eigenvalues for Co(II) centers: (a) CoO_6^{10-} cluster associated to the LS cubic $Co^{II+}(d\epsilon^6 d\gamma^1)$ center. (b) CoO_6^{10-} cluster associated to the HS cubic $Co^{2+}(d\epsilon^5 d\gamma^2)$ center. (c) and (d) CoO_5F^{9-} and CoO_5^{8-} clusters associated to the HS Co^{2+}-F and the HS Co^{2+}-V_O centers. (The small arrows on t_{2g} and e_g states picture the occupation of Co $3d$ states.)

2. Axial centers

The preceding observations hold for axial centers, but additional effects due to the presence of fluorine ions or of a vacancy site are observed. The comparison of the electronic structures associated to the axial M-X and to the cubic M centers ($M \equiv Ti^{4+}$, Co(II), Co(III), $X \equiv F, V_O$) allows us to discuss more specifically the effects of charge-compensation mechanisms.

a. Centers involving fluorine ions [Figs. 1(b) and 2(c)]. The cubic M $3d$ states are both shifted and split in MO_5F clusters. The $t_{2g} \rightarrow (e, b_2)$ and $e_g \rightarrow (a_1, b_1)$ splittings are similar but slightly stronger than in a cubic-to-tetragonal phase transition in an MO_6 cluster. When the point-group symmetry lowers, it induces additional spin-splitting effects in spin-polarized configurations: The C_{4v} occupied (↑ spin) levels are pulled down while the empty or partly filled (↓ spin) ones are slightly shifted upwards relative to the O_h corresponding states [see Figs. 2(b) and 2(c) for instance]. The case of two fluorine ions in the next vicinity of the central atom are not reported here. When the two F^- ions are substituted for oxygens along a C_4 axis (F-M-F center with D_{4h} symmetry), the resulting orbital-energy pattern is almost similar to the M one. When the two M-F axes are perpendicular, the local symmetry becomes D_{2h}, and the energy diagram is expected to be near the MO_5F one.

b. Centers with an oxygen vacancy [Figs. 1(c), 2(d), 3(c), and 3(d)]. The $X\alpha$ ground-state energy diagrams relevant to some oxygen vacancy transition-metal pair defects in cubic perovskite hosts have been given elsewhere.[17] The behaviors of Co-V_O centers are quite similar and we recall briefly the main conclusions of Ref. 17.

First, the $3d$ impurity states are shifted downwards as the metal ion moves towards the vacancy site. Simultaneously, the electronic distributions of the a_1 $d\gamma$ state show appreciable contributions of the vacancy-atomic sphere, responsible for the strong splitting (around 1 eV) between b_1 and a_1 $d\gamma$ levels. New impurity states can appear inside the band gap. This is particularly striking for Co^{III+}-V_O and Co^{3+}-V_O centers [Figs. 3(c) and 3(d)]. Indeed, in the cubic CoO_6^{9-} clusters, the $d\gamma\downarrow(Co^{3+})$ and $d\gamma(Co^{III+})$ levels lie around the CB edge, while the corresponding $d\gamma a_1$ states are localized in the middle of the gap.

Second, two levels of e and a_1 symmetries, associated to the upper O_{2p} t_{1u} cubic state, are missing in

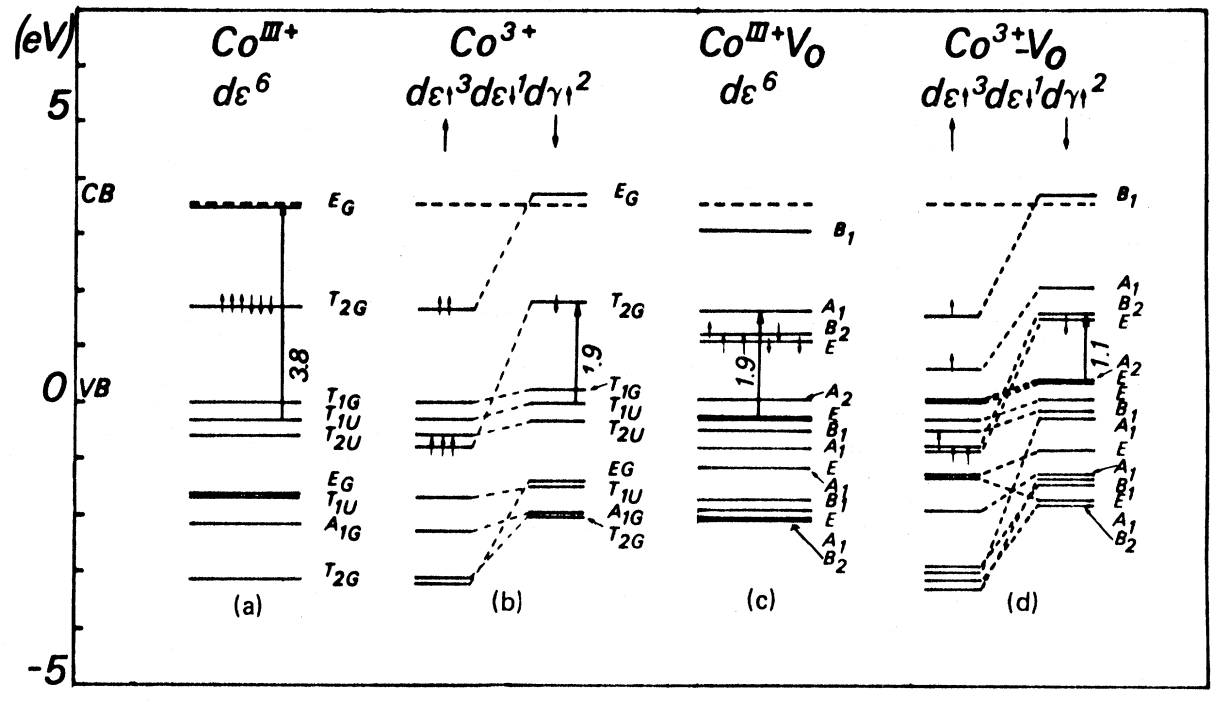

FIG. 3. Ground-state $X\alpha$ eigenvalues for Co(III) centers: (a) CoO_6^{9-} cluster associated to the LS cubic $Co^{III+}(d\epsilon^6)$ center. (b) CoO_6^{9-} cluster associated to the HS cubic $Co^{3+}(d\epsilon^4 d\gamma^2)$ center. (c) and (d) CoO_5^{7-} cluster associated to LS Co^{III+}-V_O and HS Co^{3+}-V_O axial centers.

the valence band. The t_{1g} level is split into a_2 and e states, and the cubic forbidden transition $t_{1g}\rightarrow t_{2g}$ is then allowed in C_{4v} symmetry through $e\rightarrow e$ and $e\rightarrow b_2$, $a_2\rightarrow e$ transitions, respectively, polarized parallel and perpendicular to the C_4 axis, with energies weaker than the first-allowed $t_{1u}\rightarrow t_{2g}$ cubic transition.

Third, the virtual Co 4s levels (not represented here), strongly delocalized in the extramolecular region in cubic centers, become more localized in the atomic spheres associated to the metal ion and to the vacancy in CoO_5 complexes. They lie near the empty $d\epsilon$ states and can act as electron traps to create $V_O+e(F_1)$ and $V_O+2e(F_2)$ centers.

III. OPTICAL ABSORPTION AND THEORETICAL EXCITATION ENERGIES

A. Ground-state configurations and crystal-field transitions

The optical-absorption spectra of d^n transition-metal ions usually allows one to determine the term energies and to deduce parameters like the crystal-field parameter 10Dq and the Racah's terms B and C by solving the electrostatic matrice relevant to the d^n configuration (see for instance Refs. 20 or 30). Some considerations on the TS energy diagrams or the use of approximate analytical relations as reported in Ref. 31 allow the estimation of these parameters from the knowledge of only few term energies.

In the present work, excitation energies are calculated through the transition-state procedure[32] applied to configurations suitable to obtain transitions between terms in the d^6 and d^7 configurations. The method, described by Ziegler *et al.*[33] allow us for instance to obtain the singlet-triplet and triplet-quintet splittings. We have studied the $d\epsilon^6(^1A_{1g})$, $d\epsilon^5 d\gamma(^1T_{1g}, ^1T_{2g}, ^3T_{1g}, ^3T_{2g})$, $d\epsilon^4 d\gamma^2(^5T_{2g})$, and $d\epsilon^3 d\gamma^3(^5E_g)$ configurations (terms) for Co(III), and the $d\epsilon^5 d\gamma^2(^4T_{1g})$ and $d\epsilon^6 d\gamma(^2E_g)$ configurations for Co(II). As it is not possible to separately calculate the energies of T_{1g} and T_{2g} terms inside the $d\epsilon^5 d\gamma$ configuration, we obtain averaged energies of the singlets and of the triplets, respectively, denoted $\langle E(^1T_{1g})+E(^1T_{2g})\rangle$ and $\langle E(^3T_{1g})+E(^3T_{2g})\rangle$.

In the following, $^{2s+1}\Gamma$ and $E(^{2s+1}\Gamma)$ stand for the term and its energy while ϵ_i denotes the $X\alpha$ eigenvalue of a given level i. Four parameters μ_1, μ_2, μ_3, and μ_4 are introduced in order to simplify further discussions. The appropriate relations between the $X\alpha$ eigenvalues, the term energies, and the μ parameters are reported below for each transition-state configuration.

Configuration $t_{2g\uparrow}^3 t_{2g\downarrow}^{2.5} e_{g\uparrow}^{0.5}$ of d^6:

$$\mu_1\equiv\epsilon_{e_{g\uparrow}}-\epsilon_{t_{2g\downarrow}} \equiv\langle E(^3T_{1g})+E(^3T_{2g})\rangle-E(^1A_{1g})\ . \tag{1}$$

Configuration $t_{2g\uparrow}^3 t_{2g\downarrow}^{2.5} e_{g\downarrow}^{0.5}$ of d^6:

$$\mu_2\equiv\epsilon_{e_{g\downarrow}}-\epsilon_{t_{2g\downarrow}} \equiv\tfrac{1}{2}[\langle E(^3T_{1g})+E(^3T_{2g})\rangle +\langle E(^1T_{1g})+E(^1T_{2g})\rangle]-E(^1A_{1g})\ . \tag{2}$$

Configuration $t_{2g\uparrow}^3 t_{2g\downarrow}^{1.5} e_{g\uparrow}^{1.5}$ of d^6:

$$\mu_3\equiv\epsilon_{e_{g\uparrow}}-\epsilon_{t_{2g\downarrow}} \equiv E(^5T_{2g})-\langle E(^3T_{1g})+E(^3T_{2g})\rangle\ . \tag{3}$$

Configuration $t_{2g\uparrow}^3 t_{2g\downarrow}^{0.5} e_{g\uparrow}^2 e_{g\downarrow}^{0.5}$ of d^6:

$$10\mathrm{Dq}\equiv\epsilon_{e_{g\downarrow}}-\epsilon_{t_{2g\downarrow}}\equiv E(^5E_g)-E(^5T_{2g})\ . \tag{4}$$

For the d^7 configuration, we have investigated the term splitting of $^4T_{1g}$ and ^2E_g using the transition-state configuration $t_{2g\uparrow}^3\, t_{2g\downarrow}^{2.5}\, e_{g\uparrow}^{1.5}$, we obtain

$$\mu_4\equiv\epsilon_{e_{g\uparrow}}-\epsilon_{t_{2g\downarrow}}\equiv E(^4T_{1g})-E(^2E_g)\ .$$

Equations (1)—(4) provide the ordering of the d^6 terms relative to $^1A_{1g}$.

For Co(III) trapped in $BaTiO_3$, we obtain $\mu_1=0.26$ eV, $\mu_2=1.71$ eV, $\mu_3=-0.3$ eV, $10\mathrm{Dq}=1.9$ eV. These values bring out the following conclusions: (i) The ground term is $^5T_{2g}$, but the energy difference

$$E(^5T_{2g})-E(^1A_{1g})\ ,$$

given by $\mu_1+\mu_3$, is extremely weak (0.06 eV). This corresponds to the left neighborhood of the crossover region $\mathrm{Dq}\,|\,B=2$ in the d^6 TS energy pattern. Consequently, the calculated B is around 0.095 eV. (ii) The comparison of μ_1 and μ_2 show the singlets located well above the triplets, in qualitative agreement with the TS diagram. (iii) The Dq reported above is very near of the value 1.71 eV obtained for another ferroelectric: $LaCoO_3$.[34]

The situation is somewhat different for Co(III) embedded in $SrTiO_3$. The ground term becomes $^1A_{1g}$ and the $^1A_{1g}\rightarrow{}^5T_{2g}$ splitting increases to 1.38 eV. $^5T_{2g}$ is located 0.53 eV above the averaged triplet and the singlet lies well above the quintet. This corresponds to the region around $\mathrm{Dq}\,|\,B=3$ in TS. The calculated $10\mathrm{Dq}=2.1$ eV implies that B is about 0.07 eV. The theoretical data can be compared to the values estimated from the absorption of $SrTiO_3$:Co(III).[7] The two absorption bands have been ascribed to the transitions $^1A_{1g}\rightarrow{}^1T_{1g}$ (1.77 eV)

and $^1A_{1g} \rightarrow {}^1T_{2g}$ (2.47 eV). This gives an experimental splitting

$$\langle E(^1T_{1g}) + E(^1T_{2g}) \rangle - E(^1A_{1g})$$

of 2.12 eV, slightly lower than the calculated one, $2\mu_2 - \mu_1 = 2.93$ eV. Nevertheless, the parameters $10Dq = 1.93$ eV and $B \simeq 0.08$ eV estimated by Müller[7] are of the same order as our calculated values.

The ground term of Co(II) is found to be ^2E_g in $SrTiO_3$ and $BaTiO_3$ cubic hosts, but the $^2E_g \rightarrow {}^4T_{1g}$ transition energy increases from 0.07 to 0.2 eV, from barium to strontium titanates. The preceding transition-state computations show that the terms associated to the LS and HS configurations of Co(II) and Co(III) ions have nearly equivalent energies in the $BaTiO_3$ cubic host. They point out the changes in the ground-state configurations induced by a cell-parameter variation. This is a possible explanation of the existence of LS and HS configurations in $LaCoO_3$ crystals in function of temperature.[23,24]

1. *Optical absorption of Reimeika $BaTiO_3$:Co samples*

The absorption spectra of such crystals have been reported elsewhere.[35] Two structures are present in the doped material. The first one, centered at 2.4 eV, is a broad band with an intensity increasing with the impurity percentage. The second one appears like a band-gap narrowing, with a lower limit of 2.8 eV for high Co concentration. The 2.4-eV structure disappears after reduction treatments in a hydrogen atmosphere.[9]

The 2.4-eV structure can be ascribed to charge-transfer transitions in the Co^{3+} or Co^{3+}-V_O centers [Figs. 3(b) and 3(d)]: This band is centered around the O_{2p} $t_{2u\downarrow} \rightarrow$ Co $3d$ $t_{2g\downarrow}$ transition in cubic Co^{3+} center with an $X\alpha$ excitation energy of 3 eV, which has to be compared to the 4.25-eV calculated gap for the Ti^{4+} center.[22] Three other possibilities must be discarded. (i) According to the preceding section, the crystal-field transitions are around 2 eV in $BaTiO_3$ and this is too low to account for the 2.4-eV band. (ii) It is not possible to ascribe this band to the ionization process Co(II)$\rightarrow$Co(III) by removing one electron from a Co state towards the conduction band, as it had been stated previously.[8] In fact, all clusters of Figs. 2(a)–2(d) present highest partly occupied levels below the CB state in the 0.2–0.6 eV range. Moreover, this interpretation would be incompatible with the behavior of the 2.4-eV peak under reduction. (iii) The highest occupied levels ($e_{g\uparrow}$ or $t_{2g\downarrow}$ in Co^{3+}, e_g in Co^{III+}, $b_{1\uparrow}$ in Co^{3+}-V_O) lie about 1.5 eV below the CB state. This provides a rough estimation of the energy necessary to ionize Co(III) into Co(IV) by releasing one Co $3d$ electron towards the Ti conduction band; this value appears too weak to account for the 2.4-eV band.

The band-gap narrowing can be related to Ti^{4+}-V_O centers and to all others including divalent Co ions since they exhibit partly filled or empty $3d$ states near the CB edge (see Figs. 1 and 2).

The charge-transfer transitions in all these centers induce a small amount of absorption in the blue end of the visible region. This amount increases with the Co(II) concentration, and appears in the spectra as a gap displacement towards lower energies.

2. *Photochromic bands of $SrTiO_3$:Co crystals*

The uv irradiation induces photochromic (PC) absorption bands identical to the ones obtained by oxidation, implying the photo-oxidation process Co(III)$\rightarrow$Co(IV). Simultaneously, Co(II) cubic centers are created.[6] The PC absorption bands given in Ref. 6 show two peaks centered around 1.6 and 2.6 eV. The $X\alpha$ eigenvalues of Co(IV) centers have been calculated in the HS Co^{4+} $d\epsilon^3 d\gamma^2 (^6A_{1g})$ and LS Co^{IV+} $d\epsilon\uparrow^3$ $d\epsilon\downarrow^2 (^2T_{2g})$ configurations.[36] The energy diagrams (not reported here) show that the $d\epsilon\downarrow$ and $d\gamma\downarrow$ states are shifted downwards by about 1 and 0.5 eV, respectively, as one goes from Co^{3+} to Co^{4+}. Quite similar energy lowerings are observed in the LS cases. Moreover, the Co(IV) $d\epsilon\downarrow$ level is partly filled. Consequently, the $X\alpha$ calculations predict two charge-transfer bands, due to O $2p \rightarrow$ Co(IV) $d\epsilon$ and O $2p \rightarrow$ Co(IV) $d\gamma$ transitions with energies compatible with the 1.6- and 2.6-eV experimental structures.

IV. SUMMARY

The $X\alpha$ calculations of the electronic structures of Co impurities embedded in a perovskite host give evidence for the effects of spin configurations on the molecular-orbital patterns. The theoretical investigations of the various multiplets show the possible changes of the ground term in function of the cell parameter of the crystal host.

The two structures present in the experimental-absorption spectra of Reimeika $BaTiO_3$:Co crystals are ascribed to charge-transfer transitions towards $3d$ levels of Co(III) and Co(II) cubic centers, with possible contributions of the centers arising from charge-compensation mechanisms. The optical absorption of $SrTiO_3$:Co is related to crystal-field transitions from the diamagnetic $^1A_{1g}$ ground term of Co(III) cubic center while the photochromic behavior of $SrTiO_3$:Co agrees with charge-transfer transitions implying the presence of Co(IV) cubic centers.

[1]S. A. Long and R. N. Blumental, J. Am. Ceram. Soc. 54, 515 (1971); 54, 577 (1971).
[2]G. Perluzzo and J. Destry, Can. J. Phys. 56, 453 (1978).
[3]H. J. Hagemann and H. Ihrig, Phys. Rev. B 20, 3871 (1979).
[4]B. N. Matsonashvili, Kristallografiya 12, 995 (1967) [Sov. Phys.—Crystallogr. 12, 867 (1968)].
[5]H. Ihrig, J. Phys. C 11, 819 (1978).
[6]B. W. Faughnan, Phys. Rev. B 4, 3623 (1977).
[7]K. A. Müller, in *Paramagnetic Resonances,* edited by W. Low (Academic, New York, 1963), Vol. I, p. 17.
[8]P. Caufova, H. Arend, and J. Novak, Kristallografiya 9, 113 (1964) [Sov. Phys.—Crystallogr. 9, 92 (1964)].
[9]P. Caufova, Czech. J. Phys. B 18, 1038 (1968).
[10]G. Godefroy, C. Cochet, L. Cai, and P. Jullien, J. Phys. (Paris) 36, 727, (1975).
[11]J. Voisin, Ph.D. thesis, University of Dijon, 1976 (unpublished).
[12]R. L. Berney and D. L. Cowan, Phys. B 23, 37 (1981).
[13]R. L. Wild, E. M. Rockar, and J. C. Smith, Phys. Rev. B 8, 3828 (1973).
[14]F. J. Morin and J. R. Oliver, Phys. Rev. B 8, 5847 (1973).
[15]O. F. Shirmer, W. Berlinger, and K. A. Müller, Solid State Commun. 16, 1289 (1975).
[16]F. M. Michel-Calendini and K. A. Müller, Solid State Commun. 40, 225 (1981).
[17]F. M. Michel-Calendini, Ferroelectrics 37, 499 (1981).
[18]L. F. Mattheiss, Phys. Rev. B 5, 290 (1972).
[19]D. L. Klein, G. T. Surrat and A. Barry Kunz, J. Phys. C 12, 3913 (1979).
[20]See, for example, J. S. Griffith, in *The Theory of Transition Ions* (Cambridge University Press, Cambridge, 1981) for the diagrams of Y. Tanabe and S. Sugano, J. Phys. Soc. Jpn. 9, 753 (1954).
[21]K. A. Johnson, Adv. Quantum Chem. 7, 143 (1973).
[22]F. M. Michel-Calendini, H. Chermette, and J. Weber, J. Phys. C 13, 1427 (1980).
[23]L. Richter, S. D. Bader, and M. B. Brodsky, Phys. Rev. B 22, 3059 (1980).
[24]I. G. Main, G. A. Robins, and G. Demazeau, J. Phys. C 14, 3633 (1981).
[25]K. A. Müller, Phys. Rev. B 13, 3209 (1976).
[26]E. Siegel and K. A. Müller, Phys. Rev. B 19, 109 (1979).
[27]J. G. Norman, J. Chem. Phys. 61, 4630 (1974).
[28]V. A. Gubanov, J. Weber, and J. W. D. Connolly, J. Chem. Phys. 63, 1455 (1975).
[29]K. Schwarz, Phys. Rev. B 5, 2466 (1972).
[30]S. Sugano, Y. Tanabe, and H. Kamimura, *Multiplets of Transition Metal Ions in Crystals* (Academic, New York, 1970).
[31]D. S. McClure, in *Treatise on Solid State Chemistry,* edited by N. B. Hannay (Plenum, New York, 1975), Vol. 2, p. 64.
[32]J. C. Slater, *Quantum Theory of Molecules and Solids* (McGraw-Hill, New York, 1974), Vol. 4.
[33]T. Ziegler, A. Rank, and E. J. Baerends, Theor. Chim. Acta 43, 261 (1977).
[34]R. Marx and H. Happ, Phys. Status Solidi B 67, 181 (1975).
[35]F. M. Michel-Calendini, P. Moretti, and G. Godefroy, Ferroelectrics (in press).
[36]F. M. Michel-Calendini (unpublished).